

Optical thresholding and switching using a fiber-coupled phase-conjugate mirror

R. Yahalom and A. Yariv

Department of Applied Physics, California Institute of Technology, Pasadena, California 91125

Received March 1, 1988; accepted June 22, 1988

A fiber-coupled-ring passive phase-conjugate mirror is used to achieve mutual thresholding free of bistability effects and to obtain switching among several mutually incoherent light beams.

Progress in optical computing and data processing has created a demand for all-optical switching and thresholding devices. Among the possible applications are beam steering and routing of optical signals in fiber communication networks and holographic associative-memory systems.^{1,2}

Several thresholding configurations using photorefractive crystals have been reported.³⁻⁶ These systems are limited to one signal beam and usually exhibit hysteresis behavior (bistability).

Recently it was shown⁷ that a multimode-fiber-coupled phase-conjugate mirror (PCM) can phase conjugate any input field of limited N.A., restoring the input polarization state,⁸ in the presence of both reciprocal and nonreciprocal (e.g., magnetic⁹ and amplitude¹⁰) distortions. We also demonstrated how it can be used for channeling temporal information among several mutually coherent inputs.¹¹

In this Letter we propose and demonstrate that a similar configuration can be used for an all-optical thresholding purpose, in which each of the (possibly many) input beams that are coupled to the fiber can play the role of either a signal beam or an erasure beam. The phase-conjugate signal is free of hysteresis effects, and such a device can also be used for steering (or switching) the output to different directions.¹²

The experimental setup is shown in Fig. 1. Two mutually incoherent input beams are focused into a multimode graded-index fiber (length >40 cm); each beam has an incidence angle between 0° and 10° and a separation angle $\theta < 20^\circ$. The fiber N.A. is 0.3. The N.A. of each of the input beams is approximately 0.03. The input beams are either *x* polarized or cross (*x* and

y) polarized, with no difference in the thresholding characteristics between the cases and with good recovery of the input polarization for the reflected phase-conjugate beam (because of the small input N.A., the fidelity of the restoration is ensured; see Ref. 7 and references therein for more details on this issue).

The mode-scrambled depolarized light diverging from the output end of the fiber passes through a horizontal polarizer (*p*) and is focused into a BaTiO₃-ring self-pumped PCM,¹³ with a beam diameter of 1 mm at the crystal. The phase-conjugate beam propagates backward through the fiber and then is detected by either of detectors D₁ or D₂. Detector D₃ monitors the input power at the crystal. The fiber transmittance is identical for both beams (40%).

The reflectivity of Beam 1 alone is shown in Fig. 2. It is seen that at intensities (*I*₁) smaller than approximately 2 mW/mm² the reflectivity is not saturated (owing to the effect of large dark conductivity).

The threshold behavior is demonstrated in Fig. 3. The input power of Beam 1 is held fixed (*P*₁ = 3 mW), while the power of Beam 2 (*P*₂) is increased, starting from zero. We see that as long as *P*₂ << *P*₁, only Beam 1 is phase conjugated. When *P*₂ >> *P*₁, only Beam 2 is phase conjugated. The reflected output field is a true phase conjugate of the stronger input beam, free of cross talk from the second beam. It should be emphasized that there is no *a priori* distinction between the two beams as far as the threshold behavior is concerned; the roles of *P*₁ and *P*₂ are interchangeable, and each of them can be regarded as either an erasure beam or a signal beam, depending on the specific application. It is therefore also possible to use this con-

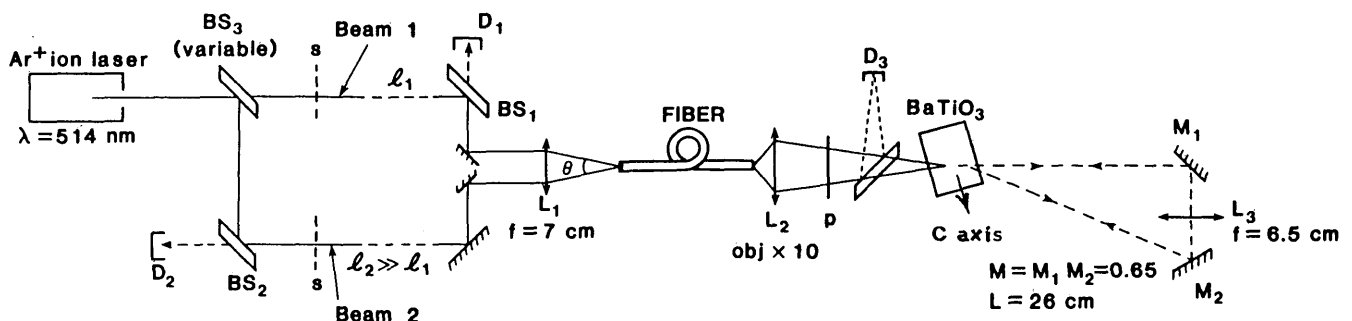


Fig. 1. Experimental setup of a two-beam thresholding device. BS's, beam splitters; L's, lenses; M's, mirrors.

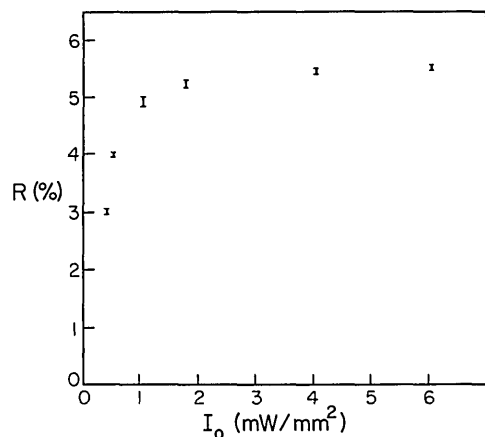


Fig. 2. Measured reflectivity of Beam 1 as a function of the input intensity to the crystal. Beam 2 is closed in this case ($P_2 = 0$).

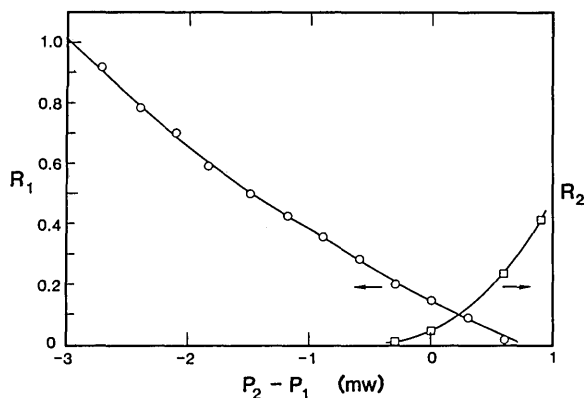


Fig. 3. Reflectivities of Beam 1 (R_1) and Beam 2 (R_2) as functions of ($P_2 - P_1$). R_1 is normalized to 1 when $P_2 = 0$, and R_2 is normalized to 1 when $P_1 = 0$.

figuration for switching purposes; the output of the system can be steered from the direction of Beam 1 to that of Beam 2 simply by changing the input ratio of the two beams. A further advantage is that it is the input power ratio, not the intensity ratio, that is important. Both beams, after propagation and intermodal scattering in the fiber, occupy the same modes, so that the interaction in the crystal is independent of the initial conditions. For example, the input beams can be of different diameters, incident from different angles, and spatially modulated. We emphasize that these properties are a direct consequence of the use of a multimode fiber, which permits the complete overlap of the different inputs while preserving the original initial conditions on reflection.

Figure 4 shows the experimental results of Beam 1 reflectivity (R_1) for several fixed values of input power P_1 as a function of the input power ratio P_2/P_1 . These results were achieved independently of the direction of change of P_2 and the initial condition. We notice that for each P_1 there is a threshold ratio beyond which the reflectivity of Beam 1 is negligible and that R_1 is almost linear in most of the cases.

Figure 5 shows the dependence of $(P_2/P_1)_{th}$ (the point where the reflectivity drops to 10% of the maximum value) on P_1 for a greater range of input powers (P_1). It is seen that the threshold ratio tends to saturate to a fixed value beyond 5-mW input power to the crystal.

The experiment was repeated with three mutually incoherent beams simultaneously coupled into the fiber. When $P_1 > P_2 + P_3$, only Beam 1 was reflected back with a full recovery of its properties, while P_2 and P_3 , being below threshold, were not reflected.

When one or more of the input beams carry spatial information, the thresholding acts globally on the whole spatial profile. Only if the total power exceeds the threshold value is this picture phase conjugated in its entire spatial structure. (The fidelity of reproduction is limited, however, by the input N.A.¹⁴ High fidelity could be obtained by using a polarization-preserving phase conjugator¹⁵ after the fiber.)

The basic features of the results shown above can be explained by a phenomenological model, according to which each beam serves as an erasure beam for the other. In the case of one uniform (plane-wave) beam, we can show that the reflectivity of a ring self-pumped PCM is given by

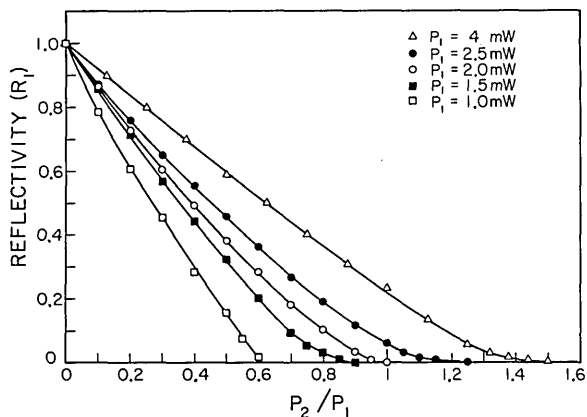


Fig. 4. Experimental results of the reflectivity of Beam 1 as a function of the input power ratio of Beam 2 to Beam 1 for several values of Beam 1 input powers (P_1). The results are normalized to 1 when $P_2 = 0$.

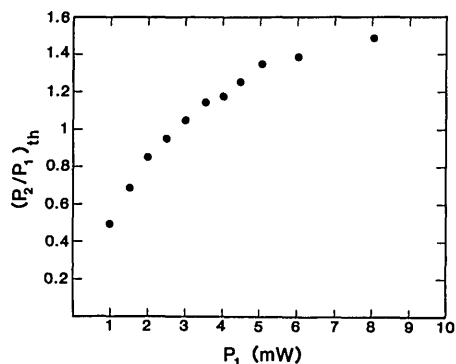


Fig. 5. Dependence of the threshold power ratio (defined in the text) as a function of Beam 1 input power (P_1).

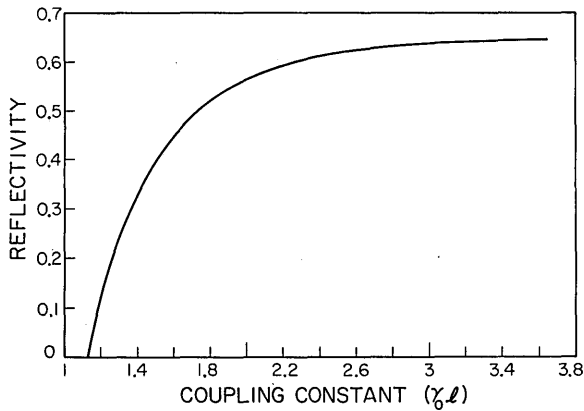


Fig. 6. Theoretical curve for a ring self-pumped PCM reflectivity as a function of the coupling constant, with $M = 0.65$ and $\sigma_d/\sigma_p \rightarrow 0$.

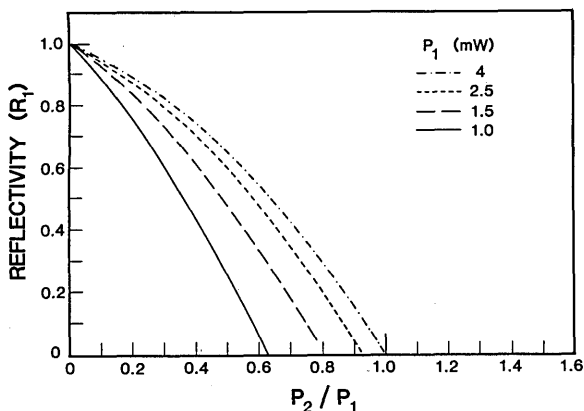


Fig. 7. Theoretical curves for the normalized reflectivities of Beam 1 as functions of Beam 1 to Beam 2 power ratio, with $M = 0.65$, $\gamma_0 l = 2.4$, and σ_d/σ_p ($P_1 = 1$ mW) = 0.5.

$$R = \frac{1}{4} \left\{ \frac{T^2(1+M)^2[1+M^{1/2}(1-T^2+MT^2)^{1/2}]}{(1+MT^2)^2} - (1-M)^2 \right\}, \quad (1)$$

where M is the feedback parameter (total round-trip loss) and

$$T = \tanh\left\{\frac{1}{2}\gamma_0 l[4R_1 + (1-M)^2]^{1/2}/(1+M)\right\}. \quad (2)$$

We assume that Beam 2 erases the grating created by Beam 1 and reduces the effective coupling,

$$\gamma_{\text{eff}} = \gamma_0/(1 + I_2 I_1 + \sigma_d/\sigma_p). \quad (3)$$

Here σ_d is the dark conductivity and σ_p ($\propto I_1$) is the photoconductivity induced by the signal beam. Figure 6 shows the theoretical reflectivity of a ring self-pumped PCM¹³ as a function of $\gamma_0 l$, when $M = 0.65$ and $\sigma_d \ll \sigma_p$. It is seen that if $\gamma_0 l$ is smaller than approximately 3, a decrease of γ leads to a decrease of the reflectivity, and the threshold value is $\gamma_{\text{th}} = 1.12$.

We can fit the threshold value and functional behavior of our data, as shown in Fig. 2, to the theoretical predictions [Eqs. (1) and (2)] if $\gamma_0 l = 2.4$ and σ_d/σ_p (I_1

= 1 mW/mm²) = 0.5. Using these values, Fig. 7 shows the theoretical predictions as given by Eqs. (1)–(3) (with $I_2 \neq 0$). By comparing Fig. 4 with Fig. 7 we can see that the simple theory can approximately recover the main features of the experimental results for $P_1 < 2$ mW. The almost linear behavior of R_1 is due to the small (<3) value of $\gamma_0 l$, as explained before in the case of $\sigma_d = 0$ (Fig. 6). The increase of $(P_2/P_1)_{\text{th}}$ with increasing P_1 is due to the nonzero contribution of σ_d/σ_p to γ_{eff} at the experimental values of P_1 (remember that σ_p depends on I_1). However, for higher values of P_1 we do not reproduce the exact threshold points, as the theoretical reflectivity is decreased much faster than the experimental results. Such behavior is thought to be due to mutual scattering, because at high powers of both beams Beam 1 can also be diffracted, to some extent, from the grating created by Beam 2.

To conclude, we have shown how a simple all-optical thresholding and switching device can be obtained by using a fiber-coupled PCM. Such a device is effective for several simultaneously coupled mutually incoherent beams; it operates on the basis of input power ratios and is robust in the sense that the operation is not sensitive to any other characteristics of the input beams.

This research is sponsored by the U.S. Army Research Office. The authors would like to acknowledge helpful discussions with A. Agranat and Y. Tomita.

References

1. H. M. Gibbs, S. L. McCall, and T. N. C. Venkatesman, *Opt. Eng.* **19**, 463 (1980); D. Psaltis and N. H. Farhat, *Opt. Lett.* **10**, 981 (1985).
2. A. Yariv, S.-K. Kwong, and K. Kyuma, *Appl. Phys. Lett.* **48**, 1114 (1986); B. H. Soffer, G. J. Dunning, Y. Owechko, and E. Marom, *Opt. Lett.* **11**, 118 (1986).
3. M. B. Klein, G. J. Dunning, G. C. Valley, P. C. Lind, and T. R. O'Meara, *Opt. Lett.* **11**, 575 (1986).
4. S.-R. Kwong and A. Yariv, *Opt. Lett.* **11**, 377 (1986).
5. S.-K. Kwong, M. Cronin-Golomb, and A. Yariv, *Appl. Phys. Lett.* **45**, 1816 (1984).
6. M. Cronin-Golomb and A. Yariv, *J. Opt. Soc. Am. A* **3**(13), P16 (1986).
7. Y. Tomita, R. Yahalom, and A. Yariv, *J. Opt. Soc. Am. B* **5**, 690 (1988).
8. K. Kyuma, A. Yariv, and S.-K. Kwong, *Appl. Phys. Lett.* **49**, 617 (1986).
9. S.-K. Kwong, R. Yahalom, and A. Yariv, *Opt. Lett.* **12**, 337 (1987).
10. Y. Tomita, K. Kyuma, R. Yahalom, and A. Yariv, *Opt. Lett.* **12**, 1020 (1987).
11. R. Yahalom, K. Kyuma, and A. Yariv, *Appl. Phys. Lett.* **52**, 292 (1987).
12. For a preliminary report of similar results, see R. Yahalom, A. Agranat, and A. Yariv, in *Technical Digest of Topical Meeting on Photonic Switching* (Optical Society of America, Washington, D.C., 1987), paper FB3.
13. M. Cronin-Golomb, B. Fischer, J. O. White, and A. Yariv, *IEEE J. Quantum Electron.* **QE-20**, 12 (1984).
14. Y. Tomita, R. Yahalom, and A. Yariv, *Opt. Lett.* **12**, 1017 (1987).
15. P. H. Beckwith, I. McMichael, and P. Yeh, *Opt. Lett.* **12**, 510 (1987).